Stable Vortex-Antivortex Molecules in Mesoscopic Superconducting Triangles

V. R. Misko,[1,*] V. M. Fomin,[1,†] J. T. Devreese,[1,‡] and V. V. Moshchalkov[2]

[1]*Theoretische Fysica van de Vaste Stoffen, Universiteit Antwerpen (U.I.A.), Universiteitsplein 1, B-2610 Antwerpen, België*
[2]*Laboratorium voor Vaste-Stoffysica en Magnetisme, Katholieke Universiteit Leuven, Celestijnenlaan 200 D, B-3001 Leuven, België*
(Received 6 March 2002; published 11 April 2003)

A thermodynamically stable vortex-antivortex pattern has been revealed in equilateral mesoscopic type I superconducting triangles, contrary to type II superconductors where similar patterns are unstable. The stable vortex-antivortex "molecule" appears due to the interplay between two factors: a repulsive vortex-antivortex interaction in type I superconductors and the vortex confinement in the mesoscopic triangle.

DOI: 10.1103/PhysRevLett.90.147003 PACS numbers: 74.20.De, 74.25.–q, 74.25.Op

Symmetrically confined vortex matter in superconductors, superfluids, and Bose-Einstein condensates offers unique possibilities to study the interplay between the C_∞ symmetry of the magnetic field and the discrete symmetry of the boundary conditions. Superconductivity in mesoscopic equilateral triangles, squares, etc., in the presence of a magnetic field nucleates by conserving the imposed symmetry (C_3, C_4) of the boundary conditions [1] and the applied vorticity. In an equilateral triangle, for example, in an applied magnetic field H generating two flux quanta, $2\Phi_0$, superconductivity appears as the C_3-symmetric combination $3\Phi_0$-Φ_0 (denoted as "3-1") of three vortices and one *antivortex* in the center. These symmetry-induced antivortices can be important not only for superconductors but also for symmetrically confined superfluids and Bose-Einstein condensates. Since the order parameter patterns reported in Refs. [1] have been obtained in the framework of the linearized Ginzburg-Landau (GL) theory, this approach is valid only close to the nucleation line $T_c(H)$. Can these novel symmetry-induced vortex-antivortex patterns then survive deep in the superconducting state? Several attempts have already been made to answer this crucial question. In the limit of an extreme type II superconductor ($\kappa \gg 1$), it has been shown that a configuration of one antivortex in the center and four vortices on the diagonals of the square is unstable away from the phase boundary [2,3]. Such a vortex state is very sensitive to any distortion of the symmetry and can easily be destroyed by a small defect set to the system [4]. Recently, the symmetry-induced solution with an antivortex has been found [5] in a thin-film superconducting square, in a broader region of the phase diagram than that in Refs. [1]. Possible scenarios of penetration of a vortex into a mesoscopic superconducting triangle with increasing magnetic field have been studied in Ref. [6]. While a single vortex enters the triangle through a midpoint of one side, a symmetric ("3-2") combination of three vortices and one antivortex with vorticity $L_{av} = -2$ turns out to be energetically favorable when the vortices are close to the center of the triangle [6].

The previous inferences on vortex-antivortex states in mesoscopic structures seem to give us no hope to find *stable* vortex-antivortex configurations deeper in the superconducting state, considering them just as the features appearing in materials with $\kappa \gg 1$ at $T_c(H)$ together with superconductivity. *Here we propose the new solution demonstrating the stability of the vortex-antivortex patterns.* This solution is based on the simple conjecture made by one of the authors (V. V. M. [7]): the main source of the vortex-antivortex pattern instability, namely, vortex-antivortex *attraction,* can be removed by taking—instead of type II—type I superconductors, where vortex-antivortex interaction becomes repulsive. Indeed, when passing through the dual point $\kappa = 1/\sqrt{2}$, the vortex-vortex interaction changes the sign [8–10] and becomes attractive at $\kappa < 1/\sqrt{2}$. At the same time, the vortex-antivortex interaction becomes repulsive. Therefore, one can expect that presence of *antivortices,* together with *confinement* of vortices and antivortices due to a potential barrier at the boundaries, can stabilize *novel vortex-antivortex patterns in a mesoscopic sample of type I superconductor.* Optimizing the geometry and the sizes of mesoscopic samples, one can therefore fulfill the conditions necessary for the existence of stable vortex-antivortex configurations. For instance, the presence of sharp corners is known [11–14] to lead to a strongly inhomogeneous distribution of the superconducting order parameter in a mesoscopic sample. Enhanced superconducting condensate density at the corners prevents vortices from leaving the sample. Together with the sign inversion of the vortex-antivortex interaction, this can stabilize novel vortex-antivortex configurations.

To verify these intuitive considerations, we investigate a mesoscopic prism of a type I superconductor with a cross section in the shape of an equilateral triangle (denoted "triangle") placed in applied magnetic field. The triangle is a proper candidate to search for stable vortex-antivortex configurations because (i) among convex simply connected figures, it has the highest enhancement factor of the critical magnetic field, and (ii) a vortex-antivortex configuration with the lowest total vorticity is expected to be stable, namely, the combination consisting of three vortices ($L_{3v} = 3$) and one antivortex with vorticity $L_{av} = -1$ (3-1 combination, or $3v + 1av$ *molecule*). (It is important to note that these vortex states are essentially beyond the model used in Ref. [15], which allows *only giant-vortex states* centered at the axis of an infinitely long cylinder.) The side of the triangle ($a = 1\ \mu$m) is taken to be larger than ξ and λ. In our calculations, the used values of the GL parameters are typical for such metals as Pb (type I): $\xi = 82$ nm, $\lambda = 39$ nm, $\kappa = 0.48$; and Nb (type II): $\xi = 39$ nm, $\lambda = 50$ nm, $\kappa = 1.28$ [16]. In this Letter, the prism is mainly supposed to be infinitely long in the z direction. We also discuss a long finite-height prism. In the limit of thin-film samples, κ_{eff} increases [3,6,13,14], and triangles behave as type II superconductors.

In the description of the superconducting properties of mesoscopic triangles, we rely upon the GL equations for the order parameter ψ and the vector potential $\mathbf{A}$ of the magnetic field $\mathbf{H} = \text{rot}\mathbf{A}$ [16–18]. In the dimensionless form, when keeping the temperature dependence explicitly, the GL equations are

$$(-i\nabla - \mathbf{A})^2\psi - \psi\left[\left(1 - \frac{T}{T_c}\right) - |\psi|^2\right] = 0, \qquad (1)$$

$$\kappa^2\Delta\mathbf{A} = \frac{i}{2}(\psi^*\nabla\psi - \psi\nabla\psi^*) + \mathbf{A}|\psi|^2. \qquad (2)$$

The imposed boundary condition is

$$\mathbf{n}\cdot(-i\nabla - \mathbf{A})\psi|_{\text{boundary}} = 0. \qquad (3)$$

Topological characteristics of solutions of the GL equations are determined by (anti)vortex core lines. One revolution along any closed path around such a line changes the phase of the order parameter by $2\pi L$, where L is the winding number (vorticity) of a vortex or antivortex. The GL Eqs. (1) and (2) with the boundary conditions are solved numerically, using the finite-difference method, on a square mesh with the density of 200 nodes per side of the triangle. The iteration procedure provides a high accuracy of calculation: the relative error for $|\psi(x,y)|^2$ is less than 10^{-4}, i.e., at least 1 order of magnitude lower than the minimal nonzero values of $|\psi(x,y)|^2$ shown in figures in the present Letter.

In order to study stability of the solutions, the calculations are performed for various values of the GL parameter κ and for various temperatures. Specific values of magnetic field are chosen to provide states with total vorticity $L = 2$ and possess a lower free energy than other states with $L = 0, 1, 3$ etc. States with total vorticity $L = 2$ can be represented by two possible configurations: (i) two vortices in the form of a multivortex or a giant-vortex state; (ii) the symmetric 3-1 combination. (Symmetric combinations with a larger number of vortices and antivortices such as "6-4," "9-7," etc., possess a higher free energy than the 3-1 combination.)

According to our calculations, it is the 3-1 combination that minimizes the free energy in case of a type I superconductor, if appropriate material and external parameters are provided. In Fig. 1, the free energy for the 3-1 combination is shown as a function of the distance d_v counted from the center of the triangle along the bisectors to vortices, for $\kappa = 0.7$, $T/T_c = 0.92$, and $H_0 = 0.72H_c(0)$, where $H_c(0)$ is the thermodynamical critical field [16,18] at zero temperature. There are three minima of the free energy as a function of d_v. The first minimum, which is at $-1.29\xi(0)$ from the center of the triangle, corresponds to a configuration when vortices are situated between the center of the triangle and the midpoints of the sides of the triangle. This is a saddle point for the free energy as a function of the coordinates (x, y) in the plane of the triangle, and the state is unstable. The second minimum is reached when all the vortices are in the center of the triangle, and the vortex-antivortex combination degenerates to a giant vortex $L_{2v} = 2$. This local minimum represents a metastable state.

The absolute minimum is reached when three vortices are situated between the center and the apexes of the triangle at $1.76\xi(0)$ from the antivortex in the center (Fig. 1). *This vortex-antivortex molecule is thermodynamically stable.* Its stability can be understood in the following way. Let us analyze the distribution of the squared modulus of the order parameter $|\psi(x,y)|^2$

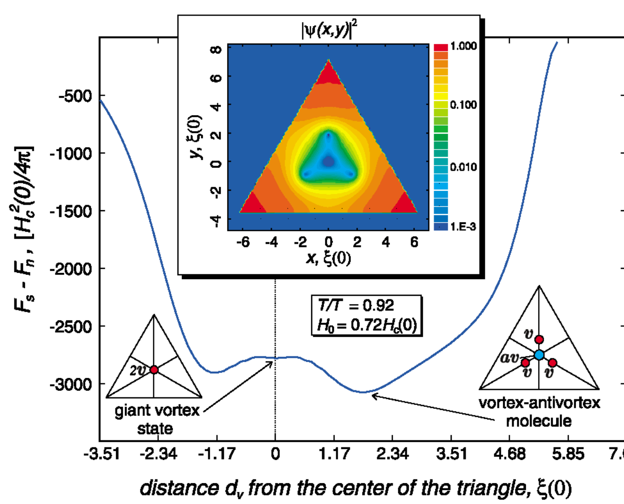

FIG. 1 (color). The free energy $F_s - F_n$ [measured in $H_c^2(0)/4\pi$] as a function of the distance d_v from the center of a mesoscopic type I superconducting triangle for the 3-1 combination, or $3v + 1av$ molecule, at $T/T_c = 0.92$, $H_0 = 0.72H_c(0)$, for $\kappa = 0.7$, $\xi(0) = 82$ nm. In the inset, the distribution of the squared modulus of the order parameter $|\psi(x,y)|^2$ is shown, which corresponds to the stable vortex-antivortex molecule.

corresponding to the above stable vortex-antivortex molecule (inset of Fig. 1). Four zeros of $|\psi(x, y)|^2$ correspond to three vortices and one antivortex. The function $|\psi(x, y)|^2$ reaches its maximum value in the corners. These "islands" of the superconducting phase in the corners prohibit vortices, which are repelled by the antivortex in the center, from leaving the triangle through the corners. Thus, vortices, being confined in a mesoscopic type I superconducting triangle and interacting with an antivortex, form a stable vortex-antivortex molecule. The stability of the vortex-antivortex molecule has been verified by analyzing the free energies of rotated and distorted molecules and of other symmetric and nonsymmetric vortex patterns with the total vorticity $L = 2$.

The obtained vortex-antivortex pattern remains stable in some range of temperatures, far away from T_c. The molecule evolves continuously when moving towards the nucleation line $T_c(H)$, as shown in Fig. 2. At low temperatures ($T/T_c = 0.90$), the free energy landscape (in the xy plane) is quite complicated, with saddle points and local minima competiting with the main minimum, which determines the stable molecule. For higher temperatures, the main minimum remains the only one. Simultaneously with the simplification of the free-energy landscape, the minimum related to the 3-1 combination moves away from the center of the triangle (cf. curves for $T/T_c = 0.94$ and $T/T_c = 0.96$). With increasing temperature, the superconducting phase in the apex regions, which "squeezes" the molecule, is suppressed and the vortices being repelled by the antivortex in the center are shifted closer to the corners.

It is worth noting that for our type I sample a strongly enhanced nucleation field appears due to the confinement of the superconducting condensate in the mesoscopic triangle. In fact, this provides the "soft" scenario for the nucleation of the order parameter, like in bulk type II superconductors. Indeed, in a mesoscopic triangle the enhancement factor $\eta = H^*_{c3}/H_{c2}$ is in general higher than its value for the surface superconductivity, $H_{c3}/H_{c2} = 1.695$ [16,18], and could increase considerably near the corners [12,14,19]. Therefore, there exists a certain region of values of $\kappa < 1/\sqrt{2}$, for which H^*_{c3} remains to be higher than H_c. The results of the free-energy calculations are shown in Fig. 3, for various values of κ close to the dual point $\kappa = 1/\sqrt{2}$. The vortex-antivortex molecule occurs to be stable for $\kappa \lesssim 1/\sqrt{2}$ (the curve for $\kappa = 0.7$ in Fig. 3). For higher values of κ, the symmetric molecule degenerates to a giant-vortex state in the center of the triangle. On the contrary, for decreasing values of κ, the molecule first rotates in such a way that vortices occur to be near the midpoints of the sides of the triangle (the curve for $\kappa = 0.6$ in Fig. 3), and then, for lower values of κ, they are pushed out from the sample. For small κ vortices do not penetrate the sample at all because the condition $H^*_{c3} > H_c$ does not fulfill, and superconductivity nucleates abruptly as in bulk type I samples.

The necessary conditions to stabilize vortex-antivortex patterns can be easier satisfied for samples finite in the z direction. In the case of a prism of finite-height h, magnetic field can penetrate the sample through the bases and form vortices. For a long finite-height prism, $h > \lambda$, magnetic field is partially expelled from the sample. This effect can be taken into account using an approach, which involves a simulation region [6,19,20]. Our calculations show that it is enough to choose a prism with a square cross section in the xy plane with the side $3a$ as a simulation region, which provides for the magnetic field at its boundaries equal to the applied field H_0. Inside the simulation region, the total magnetic flux through its cross section in the xy plane is, obviously, the same [19,20]. For long finite-height prisms, the

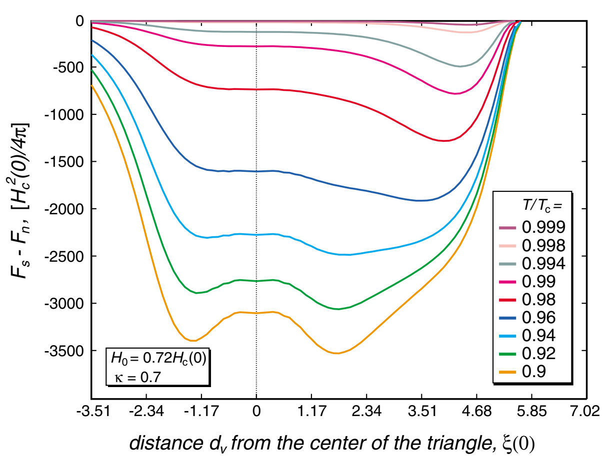

FIG. 2 (color). The free energy $F_s - F_n$ [measured in $H_c^2(0)/4\pi$] as a function of d_v for the 3-1 combination in a mesoscopic type I superconducting triangle, for $\kappa = 0.7$ [$\xi(0) = 82$ nm], $H_0 = 0.72H_c(0)$, and various temperatures.

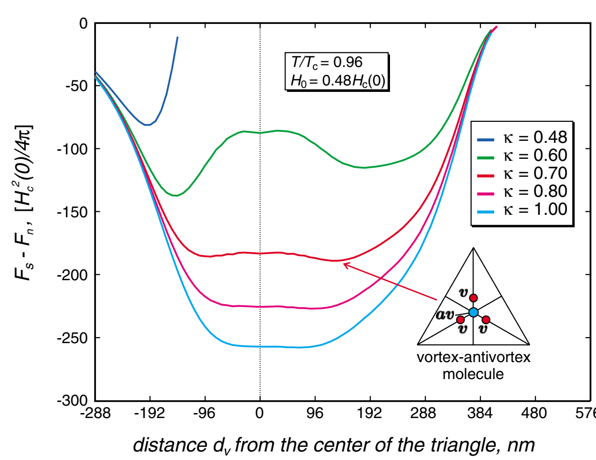

FIG. 3 (color). The free energy $F_s - F_n$ [measured in $H_c^2(0)/4\pi$] as a function of d_v for the 3-1 combination in mesoscopic type I and type II superconducting triangles, at $T/T_c = 0.96$, $H_0 = 0.48H_c(0)$, for various values of κ.

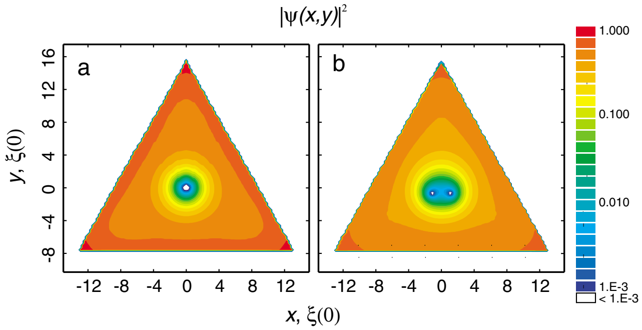

FIG. 4 (color). Typical distributions of $|\psi(x, y)|^2$ in mesoscopic type II superconducting triangles (Nb), for the states with the total vorticity $L = 2$: a giant vortex state (a); a stable multivortex state (b), at $T/T_c = 0.96$, $H_0 = 0.32 H_c(0)$.

free-energy calculations result [21] in curves similar to that plotted in Fig. 1 for an infinitely long prism. In the limit of a thin-film sample, $h \ll \lambda$, magnetic field penetrates the sample with no distortion. In this limit, the vortex-antivortex molecule appears to be stable for a wider "window" of the values of parameter κ [22]. A finite height of a sample together with the field effects appears to be favorable for the stabilization of the vortex-antivortex patterns in mesoscopic superconducting triangles.

Stable vortex-antivortex patterns are qualitatively different in case of a type II superconducting triangle. The free-energy calculations for the 3-1 combination show that the lowest minimum is reached when all the vortices are in the center of the triangle, i.e., the giant vortex with vorticity $L_{2v} = 2$ is energetically more favorable in a type II superconducting triangle than the vortex-antivortex molecule. However, the equilibrium is reached for another vortex state, which does not possess the symmetry of the sample, namely, for a state of two vortices situated at two different bisectors of the triangle (cf. Ref. [3]). Typical distributions of $|\psi(x, y)|^2$ are plotted in Fig. 4 for the giant vortex with vorticity $L_{2v} = 2$ [Fig. 4(a)] and for the stable two-vortex state in a type II superconducting triangle [Fig. 4(b)].

In conclusion, we have found deep in the superconducting state a thermodynamically *stable* vortex-antivortex configuration for a mesoscopic type I superconducting triangle, although until now it has been thought that vortex-antivortex patterns are unstable and they can manifest themselves only in the close vicinity to the phase boundary. Vortex-antivortex arrays become unstable in a type II superconducting triangle, in accordance with previous reports. The stability of the vortex-antivortex molecules in type I superconducting triangles is due to the change of the sign in the vortex-vortex and vortex-antivortex interaction forces when passing through the dual point $\kappa = 1/\sqrt{2}$, combined with the condensate confinement by the boundaries of the mesoscopic triangle.

This work has been supported by GOA BOF UA 2000, IUAP, the FWO-V Projects No. G.0306.00, No. G.0274.01, the WOG WO.025.99N (Belgium), and the ESF Programme VORTEX. Useful discussions with L. Van Look, M. Morelle, and G. Teniers are acknowledged.

*Permanent address: Institute of Applied Physics, strada Academiei 5, MD-2028 Kishinev, Republic of Moldova.
†Permanent address: State University of Moldova, strada A. Mateevici, 60, MD-2009 Kishinev, Republic of Moldova.
‡Also at Universiteit Antwerpen (RUCA), Groenenborgerlaan 171, B-2020 Antwerpen, België and Technische Universiteit Eindhoven, P.O. Box 513, 5600 MB Eindhoven, The Netherlands.

[1] L. F. Chibotaru, A. Ceulemans, V. Bruyndoncx, and V. V. Moshchalkov, Nature (London) **408**, 833 (2000); Phys. Rev. Lett. **86**, 1323 (2001).
[2] J. Bonča and V. V. Kabanov, Phys. Rev. B **65**, 012509 (2002); V. M. Vinokur (unpublished).
[3] B. J. Baelus and F. M. Peeters, Phys. Rev. B **65**, 104515 (2002).
[4] A. S. Mel'nikov, I. M. Nefedov, D. A. Ryzhov, I. A. Shereshevskii, V. M. Vinokur, and P. P. Vysheslavtsev, Phys. Rev. B **65**, 140503 (2002).
[5] T. Mertelj and V. V. Kabanov, cond-mat/0212274.
[6] V. R. Misko, V. M. Fomin, J. T. Devreese, and V. V. Moshchalkov, Physica (Amsterdam) **369C**, 361 (2002).
[7] V. V. Moshchalkov (unpublished).
[8] E. H. Brandt, J. Low Temp. Phys. **53**, 41 (1983).
[9] A. Brass and H. J. Jensen, Phys. Rev. B **39**, 9587 (1989).
[10] F. Mohamed, M. Troyer, G. Blatter, and I. Luk'yanchuk, cond-mat/0201499.
[11] A. Houghton and F. B. McLean, Phys. Lett. **19**, 172 (1965).
[12] V. M. Fomin, J. T. Devreese, and V. V. Moshchalkov, Europhys. Lett. **42**, 553 (1998); **46**, 118 (1999).
[13] V. V. Moshchalkov, L. Gielen, C. Strunk, R. Jonckheere, X. Qiu, C. Van Haesendonck, and Y. Bruynseraede, Nature (London) **373**, 319 (1995).
[14] V. M. Fomin, V. R. Misko, J. T. Devreese, and V. V. Moshchalkov, Solid State Commun. **101**, 303 (1997); Phys. Rev. B **58**, 11 703 (1998).
[15] G. F. Zharkov, Phys. Rev. B **63**, 224513 (2001).
[16] C. P. Poole, Jr., H. A. Farach, and R. J. Creswich, *Superconductivity* (Academic Press, San Diego, 1995).
[17] V. L. Ginzburg and L. D. Landau, Zh. Eksp. Teor. Fiz. **20**, 1064 (1950).
[18] M. Tinkham, *Introduction to Superconductivity* (McGraw-Hill, New York, 1996), 2nd ed.
[19] V. R. Misko, V. M. Fomin, and J. T. Devreese, Phys. Rev. B **64**, 014517 (2001).
[20] P. Singha Deo, V. A. Schweigert, F. M. Peeters, and A. K. Geim, Phys. Rev. Lett. **79**, 4653 (1997).
[21] V. R. Misko, V. M. Fomin, J. T. Devreese, and V. V. Moshchalkov, cond-mat/0203140.
[22] V. R. Misko, V. M. Fomin, J. T. Devreese, and V. V. Moshchalkov (to be published).